ELSEVIER

Carbohydrate Research 337 (2002) 1485–1493

CARBOHYDRATE RESEARCH

www.elsevier.com/locate/carres

Sugar interaction with metal ions. The coordination behavior of neutral galactitol to Ca(II) and lanthanide ions

Limin Yang, Yunlan Su, Wei Liu, Xianglin Jin, Jinguang Wu*

The State Key Laboratory of Rare Earth Materials Chemistry and Applications, Department of Chemical Biology, College of Chemistry and Molecular Engineering, Peking University, Beijing 100871, PR China

Abstract

The crystal structures of $CaCl_2$·galactitol·4 H_2O and $2EuCl_3$·galactitol·14 H_2O were determined to compare the coordination behavior of Ca and lanthanide ions. The crystal system of the Ca–galactitol complex, $CaCl_2·C_6H_{14}O_6·4$ H_2O, is monoclinic, *Cc* space group. Each Ca ion is coordinated to eight oxygen atoms, four from two galactitol molecules and four from water molecules. Galactitol provides O-2, -3 to coordinate to one Ca^{2+}, and O-4, -5 with another Ca^{2+}, to form a chain structure. The crystal system of the Eu–galactitol complex, $2EuCl_3·C_6H_{14}O_6·14$ H_2O, is triclinic, $P\bar{1}$ space group. Each Eu ion is coordinated to nine oxygen atoms, three from an alditol molecule and six from water molecules. Each galactitol provides O-1, -2, -3 to coordinate with one Eu^{3+} and O-4, -5, -6 with another Eu^{3+}. The other water molecules are hydrogen-bonded in the structure. The similar IR spectra of Pr–, Nd–, Sm–, Eu–, Dy–, and Er–galactitol complexes show that those lanthanide ions have the same coordination mode to neutral galactitol. The Raman spectra also confirm the formation of metal ion–carbohydrate complexes.

Keywords: Crystal structure; FT-IR; Ca–galactitol complex; Raman; Lanthanide ions

1. Introduction

Metal–carbohydrate interactions are of interest because of their fundamental importance in many biochemical processes, such as toxic metal metabolism, the transport and storage of metals, the function and regulation of metalloenzymes, the mechanism of action of metal-containing pharmaceuticals, Ca(II)-mediated carbohydrate–protein binding, and so on.[1–3] They also implicate metallohosts derived from the assembly of sugars around metal ions.[4] Because of their structural variety, alditol and low molecular weight carbohydrates, and oligo- and polysaccharides, are versatile building blocks for the systematic synthesis of complex structures. The formation of metal–carbohydrate complexes is not only useful in separation and analysis of chiral compounds, but also in stoichimetric or catalytic stereoselective syntheses. In aqueous solution, metal ions coordinate with water molecules, and the un-ionized hydroxyl groups of carbohydrates are weak competitors for metal ion coordination. Therefore, although coordination chemistry plays a central role in these processes, carbohydrate–metal complexes are still poorly understood, and relatively few well-characterized complexes of metal ions with carbohydrate ligands have been reported, especially those lacking anchor groups.

Calcium ions and sugars appear to participate in a variety of biological adhesion and agglutination processes, including those occurring at cell surfaces.[5] Some crystalline adducts of sugars and calcium salts have been isolated and characterized by X-ray crystallography.[6,7] Galactitol is a metabolic product of galactose, but although several lanthanide–galactitol complex structures have been reported, the crystal structure of the Ca–galactitol complex is still undetermined.[8–10] We report here on the successful crystallization from aqueous solution and the structure characterization of $CaCl_2$·galactitol·4 H_2O, $2EuCl_3$·galactitol·14 H_2O, $2DyCl_3$·galactitol·14 H_2O and $2ErCl_3$·galactitol·14 H_2O by using FT-IR, FT-Raman, and especially X-ray single crystal diffraction for $CaCl_2$·galactitol·4 H_2O and

* Corresponding author. Tel.: +86-10-62757951; fax: 86-10-62751708

E-mail address: wjg@chem.pku.edu.cn (J. Wu).

0008-6215/02/$ - see front matter
PII: S0008-6215(02)00130-1

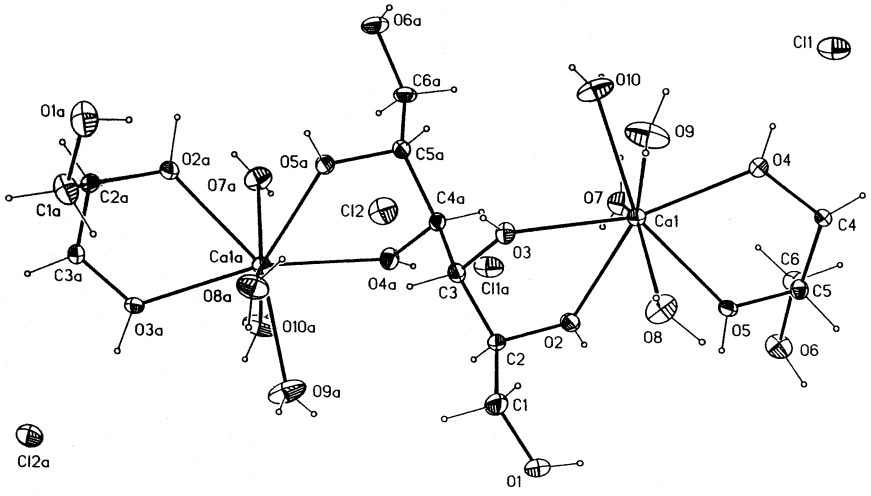

Fig. 1. The structure and atom numbering scheme of $CaCl_2{\cdot}C_6H_{14}O_6{\cdot}4\ H_2O$.

$2EuCl_3$·galactitol·14 H_2O. The IR and Raman results are consistent with the crystal structures.

2. Experimental

Materials.—$CaCl_2{\cdot}6\ H_2O$(AR) and galactitol ($C_6H_{14}O_6$, AR) were commercial products and were used as supplied. $EuCl_3$, $TbCl_3$ were prepared from the corresponding rare earth oxides of high purity (99.99%).

Preparation of galactitol complexes.—Galactitol (3 mmol, 0.54 g) and 6 mmol metal chlorides were dissolved in a water–EtOH mixture, heated to make concentrated solutions. Gradual evaporation of the solutions, cooled down to room temperature allowed crystallization. Galactitol is in neutral form in these complexes. Anal. Calcd for $CaCl_2{\cdot}C_6H_{14}O_6{\cdot}4\ H_2O$: C, 19.73; H, 6.07. Found: C, 19.09; H, 6.02. Anal. Calcd for $2EuCl_3{\cdot}C_6H_{14}O_6{\cdot}14\ H_2O$: C, 7.58; H, 4.45. Found: C, 7.510; H, 4.09.

Physical measurement.—The structure of $CaCl_2{\cdot}C_6H_{14}O_6{\cdot}4\ H_2O$ was determined on a Rigaku R-AXIS RAPID IP diffractometer using monochromized Mo Kα radiation ($\lambda = 0.71073$ Å) in the θ range from 2.90 to 27.48° at 293 K. The final cycle of full-matrix least-square refinement was based on 1750 observed reflections. The structure of $2EuCl_3{\cdot}C_6H_{14}O_6{\cdot}14\ H_2O$ was determined on the same diffractometer and radiation in the θ range from 2.07 to 27.48° at 293 K. The final cycle of full-matrix least-square refinement was based on 3427 observed reflections. Calculations were completed with the SHELX-97 program. The micro-IR spectra of $CaCl_2{\cdot}C_6H_{14}O_6{\cdot}4\ H_2O$, $2EuCl_3$·galactitol·14 H_2O, $2DyCl_3$·galactitol·14 H_2O and $2ErCl_3$·galactitol·14 H_2O ($4000–650\ cm^{-1}$) were recorded on a Nicolet Magna-IR 750 spectrometer, with 128 scans at 4 cm^{-1} resolution. The Raman spectra of Ca–galactitol and Eu–galactitol complexes ($3700–100\ cm^{-1}$) were collected on a Nicolet FT-Raman 950 spectrometer and 1000 scans at 8 cm^{-1} resolution.

3. Results and discussion

X-Ray crystal structure.—The structure and atom numbering scheme is shown in Figs. 1 and 2 is the projection of the crystal cell in the crystal structure of

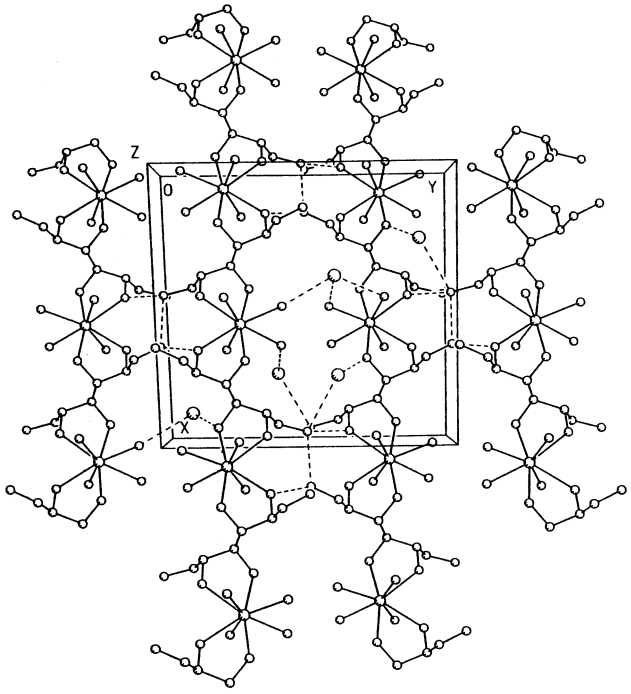

Fig. 2. The projection of the crystal cell in the crystal structure of $CaCl_2{\cdot}C_6H_{14}O_6{\cdot}4\ H_2O$.

Table 1
Crystal data and structure refinement of $CaCl_2 \cdot C_6H_{14}O_6 \cdot 4\ H_2O$

Formula weight	365.22
Temperature (K)	293(2)
Wavelength (Å)	0.71073
Crystal system, space group	monoclinic, *Cc*
Unit cell dimensions	
a (Å)	13.7612(6)
b (Å)	14.0630(5)
c (Å)	8.2001(4)
α (°)	90
β (°)	105.598(2)
γ (°)	90
V (Å^3)	1528.5(1)
Z, D_{Calc} (Mg/m^3)	4, 1.587
Absorption coefficient (mm^{-1})	0.799
$F(000)$	768
Crystal size (mm)	$0.50 \times 0.25 \times 0.15$
θ range for data collection (°)	2.90–27.48
Index ranges	$-17 \le h \le 17$, $-18 \le k \le 18$, $-10 \le l \le 10$
Reflections collected/unique	6992/1750 [$R_{int} = 0.0461$]
Completeness to $2\theta = 27.48$ (%)	49.8
Refinement method	full-matrix least-squares on F^2
Data/restraints/parameters	1750/2/216
Goodness-of-fit on F^2	1.058
Final R indices [$I > 2\sigma(I)$]	$R_1 = 0.0249$, $wR_2 = 0.0602$
R indices (all data)	$R_1 = 0.0302$, $wR_2 = 0.0617$
Absolute structure parameter	0.05(4)
Extinction coefficient	0.0331(14)
Largest difference peak and hole (e/Å^3)	0.357 and −0.396

$CaCl_2 \cdot$galactitol$\cdot 4\ H_2O$. Crystal data are listed in Table 1. Atomic parameters of $CaCl_2 \cdot$galactitol$\cdot 4\ H_2O$ are given in Table 2. Selected bond lengths and bond angles are collected in Table 3. The crystal system is monoclinic, *Cc* space group. Each Ca ion is coordinated to two galactitol molecules. One galactitol molecule chelates the calcium through the O-2, O-3 pair of hydroxyl groups, and the second molecule chelates the calcium ion through the O-4, O-5 pair of hydroxyl groups. The coordination polyhedron around the calcium is completed by four water molecules. Therefore, the calcium ion is coordinated to eight oxygen atoms: four from hydroxyl groups and four from water molecules. The Ca–O distances are from 2.414 to 2.542 Å. The average Ca–Oo (Oo is the oxygen atom of sugar a hydroxyl group) distance is 2.429 Å; the average Ca–Ow (Ow is the oxygen atom of water molecules) distance is 2.4915 Å. The data show that the average Ca–Oo distance is shorter than the average Ca–Ow distance. For galactitol, it provides O-2, -3 to coordinate with one Ca^{2+}, and O-4, -5 to coordinate with another Ca^{2+}, thus calcium cations link the carbohydrates together and a chain structure is formed. Chloride ions do not coordinate to calcium cations directly, but participate in forming extensive hydrogen bonds networks between hydroxyl groups, water molecules, and chloride ions. Hydrogen-bond data for $CaCl_2 \cdot$galactitol$\cdot 4\ H_2O$ are listed in Table 4, including three O···O and eleven O···Cl hydrogen bonds. From an examination of the crystal structures of calcium–carbohydrate salts and complexes, the general features have been deduced:[6,7] Ca^{2+} often coordinates with two or more sugars, one to four water molecules coordinate to Ca^{2+}, the coordination number of Ca^{2+} is high, the calcium–ligand distances generally fall within the range of 2.3–2.6 Å, and chloride ions do not participate in coordination. This new result for $CaCl_2 \cdot$galactitol$\cdot 4\ H_2O$ is still consistent with the rule.

Lanthanide ions are often used as a probe of Ca^{2+} to detect the bonding position of Ca^{2+} to bio-macromolecules. Although the interactions between lanthanide ions and carbohydrates have been studied by NMR, TLC, paper electrophoresis, HPLC, and elemental analysis, relatively few single-crystal structures have been determined.[11–13] The first lanthanide–carbohydrate crystal structure ($2PrCl_3 \cdot$galactitol$\cdot 14\ H_2O$) was determined only ten years ago in 1993, by Angyal.[8]

Table 2
Atomic coordinates ($\times 10^4$) and U_{eq} for $CaCl_2 \cdot C_6H_{14}O_6 \cdot 4\ H_2O$ (Å$^2 \times 10^3$)

	x	y	z	U_{eq}
Ca-1	585(1)	2247(1)	2460(1)	19(1)
Cl-1	−1149(1)	999(1)	−3632(1)	41(1)
Cl-2	2456(1)	1028(1)	8565(1)	33(1)
O-1	1403(2)	4981(2)	6139(4)	48(1)
O-2	1525(2)	3677(2)	3550(3)	23(1)
O-3	1885(2)	2072(2)	5127(3)	21(1)
O-4	−713(2)	1947(2)	−156(3)	25(1)
O-5	−453(2)	3604(2)	1299(3)	22(1)
O-6	−510(2)	4945(2)	−1419(3)	36(1)
O-7	1531(2)	2785(2)	353(4)	37(1)
O-8	−371(2)	2727(2)	4538(4)	39(1)
O-9	−45(3)	811(3)	3444(5)	51(1)
O-10	1373(3)	881(2)	1568(5)	45(1)
C-1	1859(3)	4070(3)	6517(5)	35(1)
C-2	2301(2)	3721(2)	5110(4)	21(1)
C-3	2722(2)	2718(2)	5481(4)	20(1)
C-4	−1569(2)	2567(2)	−590(4)	18(1)
C-5	−1209(2)	3586(2)	−291(4)	20(1)
C-6	−778(2)	3956(2)	−1687(5)	26(1)

U_{eq} is defined as one third of the trace of the orthogonalized U_{ij} tensor.

Table 3
Bond length (Å) and angles (°) for $CaCl_2 \cdot C_6H_{14}O_6 \cdot 4\ H_2O$

Bond lengths			
Ca-1–O-10	2.414(3)	O-3–C-3	1.434(4)
Ca-1–O-9	2.420(4)	O-4–C-4	1.432(4)
Ca-1–O-5	2.420(2)	O-5–C-5	1.432(4)
Ca-1–O-2	2.428(2)	O-6–C-6	1.441(4)
Ca-1–O-4	2.431(3)	C-1–C-2	1.523(5)
Ca-1–O-3	2.437(3)	C-2–C-3	1.524(4)
Ca-1–O-8	2.509(3)	C-3–C-4 # 1	1.531(3)
Ca-1–O-7	2.542(3)	C-4–C-5	1.515(5)
O-1–C-1	1.424(5)	C-4–C-3 # 2	1.531(3)
O-2–C-2	1.430(4)	C-5–C-6	1.516(5)
Bond angles			
O-10–Ca-1–O-9	70.56(9)	O-5–Ca-1–O-7	81.61(9)
O-10–Ca-1–O-5	140.71(12)	O-2–Ca-1–O-7	71.57(10)
O-9–Ca-1–O-5	124.24(13)	O-4–Ca-1–O-7	80.85(10)
O-10–Ca-1–O-2	122.15(11)	O-3–Ca-1–O-7	104.66(9)
O-9–Ca-1–O-2	140.52(12)	O-8–Ca-1–O-7	147.11(7)
O-5–Ca-1–O-2	72.03(6)	C-2–O-2–Ca-1	124.08(19)
O-10–Ca-1–O-4	82.96(12)	C-3–O-3–Ca-1	118.26(19)
O-9–Ca-1–O-4	84.54(13)	C-4–O-4–Ca-1	118.3(2)
O-5–Ca-1–O-4	64.79(9)	C-5–O-5–Ca-1	123.47(19)
O-2–Ca-1–O-4	131.39(9)	O-1–C-1–C-2	111.5(3)
O-10–Ca-1–O-3	84.83(11)	O-2–C-2–C-1	109.7(3)
O-9–Ca-1–O-3	81.89(13)	O-2–C-2–C-3	106.9(2)
O-5–Ca-1–O-3	130.25(8)	C-1–C-2–C-3	110.8(3)
O-2–Ca-1–O-3	64.13(8)	O-3–C-3–C-2	107.7(2)
O-4–Ca-1–O-3	164.16(6)	O-3–C-3–C-4 # 1	108.6(2)
O-10–Ca-1–O-8	141.25(11)	C-2–C-3–C-4 # 1	113.2(2)
O-9–Ca-1–O-8	72.40(11)	O-4–C-4–C-5	108.9(2)
O-5–Ca-1–O-8	72.16(10)	O-4–C-4–C-3 # 2	107.9(2)
O-2–Ca-1–O-8	81.52(9)	C-5–C-4–C-3 # 2	112.7(2)
O-4–Ca-1–O-8	104.55(10)	O-5–C-5–C-6	110.2(2)
O-3–Ca-1–O-8	79.07(9)	O-5–C-5–C-4	106.8(2)
O-10–Ca-1–O-7	71.15(11)	C-6–C-5–C-4	112.3(3)
O-9–Ca-1–O-7	140.31(11)	O-6–C-6–C-5	110.6(3)

Symmetry transformations used to generate equivalent atoms: # 1 $x+1/2$, $-y+1/2$, $z+1/2$; # 2 $x-1/2$, $-y+1/2$, $z-1/2$.

Subsequently the crystal structures of some lanthanide ions complexed with *myo*-inositol or D-ribose were reported.[14–16] In the crystal structure of $PrCl_3 \cdot$D-ribose$\cdot 5\ H_2O$, a chloride ion also coordinates to the metal ion and the ring oxygen does not participate in coordination.[16] For the $EuCl_3$–galactitol complex, a previous assignment by Angyal from elemental analysis was $EuCl_3 \cdot C_6H_{14}O_6 \cdot 3\ H_2O$ (1:1 M:L).[8] Here a 2:1 Eu^{3+}:galactitol single crystal was obtained. The Eu ion environment in the galactitol complex is depicted in Fig. 3. The crystal system is triclinic system, $P\bar{1}$ space group. Each Eu^{3+} is coordinated to nine oxygen atoms, three from the alditol and six from water molecules; each galactitol provides O-1, -2, -3 to coordinate with one Eu^{3+} and O-4, -5, -6 with another Eu^{3+} ion. Another two water molecules are hydrogen bonded in the structure and thus the formula is $2EuCl_3 \cdot$galactitol$\cdot 14\ H_2O$. Although they have different *f* electrons, Pr^{3+}, Nd^{3+}, Sm^{3+}, and Eu^{3+} ions all have the same coordination mode to galactitol.[8–10] Fig. 4 is the projection of the unit cell in the crystal structure. Crystal data are listed in Table 5. Atomic parameters of $2EuCl_3 \cdot$galactitol$\cdot 14\ H_2O$ are given in Table 6. Selected bond lengths and bond angles are collected in Table 7. Hydrogen-bond data of $2EuCl_3 \cdot$galactitol$\cdot 14\ H_2O$ are

Table 4
Hydrogen bonds with $H\cdots A < r(A) + 2.000$ Å and $\angle DHA > 110°$ for $CaCl_2 \cdot C_6H_{14}O_6 \cdot 4\ H_2O$

D–H···A	d(D–H)	d(H···A)	d(D···A)	∠(DHA)
O-1–H-11···O-6 # 3	0.76(5)	2.14(5)	2.893(4)	167(6)
O-2–H-12···O-1 # 4	1.00(6)	1.74(6)	2.705(4)	163(6)
O-3–H-13···Cl-2	0.93(7)	2.22(7)	3.087(3)	155(5)
O-4–H-14···Cl-1	0.90(8)	2.18(8)	3.056(3)	164(5)
O-5–H-15···O-6 # 3	0.79(7)	2.06(7)	2.784(4)	153(7)
O-6–H-16···Cl-2 # 5	0.90(6)	2.33(5)	3.183(3)	156(5)
O-7–H-17A···Cl-2 # 6	0.97(7)	2.36(7)	3.298(3)	162(6)
O-7–H-17B···Cl-1 # 1	0.65(7)	2.93(6)	3.519(3)	153(7)
O-8–H-18A···Cl-1 # 7	0.76(8)	2.45(8)	3.188(3)	164(7)
O-8–H-18B···Cl-2 # 2	0.88(7)	2.52(7)	3.371(3)	164(6)
O-9–H-19A···Cl-1 # 8	0.79(7)	2.44(7)	3.208(4)	164(6)
O-9–H-19B···Cl-1 # 7	0.75(8)	2.43(8)	3.176(4)	169(7)
O-10–H-20A···Cl-2 # 9	0.73(7)	2.59(7)	3.286(3)	162(7)
O-10–H-20B···Cl-2 # 6	0.73(8)	2.50(8)	3.210(4)	165(6)

Symmetry transformations used to generate equivalent atoms: # 1 $x+1/2$, $-y+1/2$, $z+1/2$; # 2 $x-1/2$, $-y+1/2$, $z-1/2$; # 3 x, $-y+1$, $z+1/2$; # 4 x, $-y+1$, $z-1/2$; # 5 $x-1/2$, $y+1/2$, $z-1$; # 6 x, y, $z-1$; # 7 x, y, $z+1$; # 8 x, $-y$, $z+1/2$; # 9 x, $-y$, $z-1/2$.

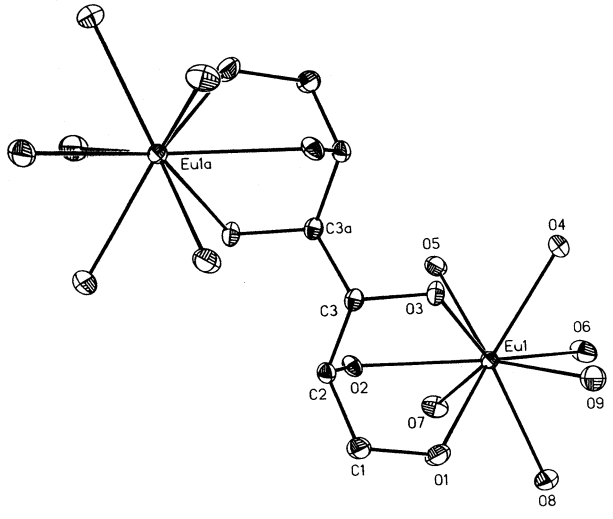

Fig. 3. The structure and atom numbering scheme of $2EuCl_3 \cdot C_6H_{14}O_6 \cdot 14\ H_2O$. (The designations C3a, O4, O5, O6 are arbitrary and do not conform to conventional sugar numbering.)

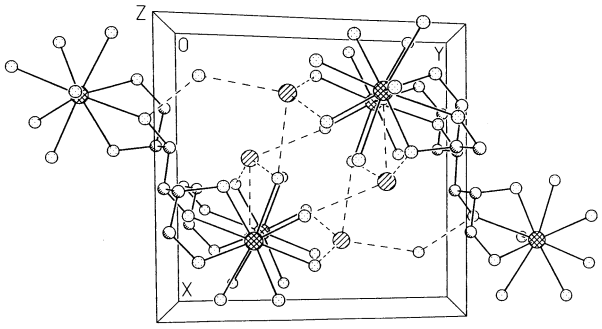

Fig. 4. The projection of the crystal cell in the crystal structure of $2EuCl_3 \cdot C_6H_{14}O_6 \cdot 14\ H_2O$.

Table 5
Crystal data and structure refinement of $2EuCl_3 \cdot C_6H_{14}O_6 \cdot 14\ H_2O$

Formula weight	951.02
Temperature (K)	293(2)
Wavelength (Å)	0.71073
Crystal system, space group	triclinic, $P\bar{1}$
Unit cell dimensions	
a (Å)	9.680(2)
b (Å)	10.342(2)
c (Å)	7.990(2)
α (°)	107.99(3)
β (°)	92.69(3)
γ (°)	88.46(3)
V (Å^3)	759.9(3)
Z, D_{Calc} (Mg/m^3)	1, 2.078
Absorption coefficient (mm^{-1})	4.687
$F(000)$	466
Crystal size (mm)	$0.60 \times 0.50 \times 0.40$
θ range for data collection (°)	2.07–27.48
Index ranges	$0 \le h \le 12$, $-13 \le k \le 13$, $-10 \le l \le 10$
Reflections collected/unique	3427/3427 [$R_{int} = 0.0000$]
Completeness to $2\theta = 27.48$ (%)	98.3
Refinement method	full-matrix least-squares on F^2
Data/restraints/parameters	3427/3/206
Goodness-of-fit on F^2	0.761
Final R indices [$I > 2\sigma(I)$]	$R_1 = 0.0210$, $wR_2 = 0.0498$
R indices (all data)	$R_1 = 0.0284$, $wR_2 = 0.0561$
Extinction coefficient	0.0242(7)
Largest difference peak and hole (e/Å^3)	1.013 and −1.263

listed in Table 8. Eu–O distances are from 2.412 to 2.515 Å. According to data in the literature,[8–10] the average Ln–Oo, Ln–Ow, Ln–O distances are as follows: Pr–Oo, 2.530 Å; Pr–Ow, 2.495 Å; Pr–O, 2.506 Å; Nd–Oo, 2.515 Å; Nd–Ow, 2.479 Å; Nd–O, 2.491 Å; Sm–Oo, 2.484 Å; Sm–Ow, 2.440 Å; Sm–O, 2.455 Å; Eu–Oo, 2.478 Å; Eu–Ow, 2.434 Å; and Eu–O, 2.449 Å. The average M–O distances are Pr–Oo > Nd–Oo > Sm–Oo > Eu–Oo; Pr–Ow > Nd–Ow > Sm–Ow > Eu–Ow; and Pr–O > Nd–O > Sm–O > Eu–O. These are consistent with the sequence of ion radius and electrons of lanthanide ions.

The carbon-chain conformation of galactitol is extended.[17] Although the conformation of galactitol is still extended after coordination to Ca or Pr, Nd, Sm, and Eu ions, it is changed, especially in the metal-ion chelate positions, and thus the C-2–O-2, C-3–O-3, C-2–C-3 bond distances are changed, and C-1–C-2–O-2, O-2–C-2–C-3, C-2–C-3–O-3 bond angles become narrower as compared to the structure of galactitol.[18] The O-1–C-1–C-2 angle becomes narrower in the lanthanide complex structure, but broader in the Ca-complex structure, because O-1 participates in coordination for the lanthanide complex, and does not coordinate to Ca^{2+}. After complexation, hydrogen bond networks formed by hydroxyl groups, water molecules, and chloride ions rearrange and become more extensive as compared with free galactitol. The crystal structure results show that galactitol adopts different modes to coordinate with Ca and lanthanide ions.

IR spectroscopy study of Ca–, Eu–, Dy–, and Er–galactitol complexes.—Pr^{3+}–, Nd^{3+}–, and Sm^{3+}–galactitol complexes have similar IR spectra and the single crystal structure results show the same coordination mode.[8–10] The IR results are thus consistent with the crystal structure results, and the similar IR spectra

Table 6
Atomic coordinates ($\times 10^4$) and equivalent isotropic displacement parameters (Å$^2 \times 10^3$) for $2EuCl_3 \cdot C_6H_{14}O_6 \cdot 14\ H_2O$

	x	y	z	U_{eq}
Eu-1	2494(1)	7105(1)	3566(1)	18(1)
Cl-1	4611(1)	2629(1)	1433(1)	33(1)
Cl-2	245(1)	2214(1)	1303(1)	38(1)
Cl-3	7615(1)	5919(1)	2786(1)	39(1)
O-1	1833(3)	8829(3)	2025(5)	40(1)
O-2	4401(3)	8028(2)	2286(3)	23(1)
O-3	3326(3)	9334(3)	5264(3)	24(1)
O-4	2501(3)	7338(3)	6697(4)	34(1)
O-5	4683(3)	6311(3)	4490(4)	31(1)
O-6	1608(4)	5048(3)	3929(4)	40(1)
O-7	3437(3)	5372(3)	1103(4)	33(1)
O-8	564(3)	6256(3)	1462(4)	33(1)
O-9	374(3)	8286(4)	4909(4)	39(1)
O-10	1895(5)	11226(4)	7593(6)	56(1)
C-1	2849(4)	9712(4)	1732(5)	30(1)
C-2	4212(4)	9471(3)	2612(4)	21(1)
C-3	4282(3)	10073(3)	4593(4)	20(1)

U_{eq} is defined as one third of the trace of the orthogonalized U_{ij} tensor.

Table 7
Selected bond lengths (Å) and angles (°) for $2EuCl_3 \cdot C_6H_{14}O_6 \cdot 14\ H_2O$

O-10–Ca-1–O-2	141.25(11)	C-2–C-3–C-4 # 1	113.20(20)
Bond lengths			
Eu-1–O-7	2.412(3)	Eu-1–O-1	2.515(3)
Eu-1–O-5	2.417(3)	O-1–C-1	1.434(5)
Eu-1–O-6	2.419(3)	O-2–C-2	1.441(4)
Eu-1–O-3	2.422(3)	O-3–C-3	1.438(4)
Eu-1–O-4	2.438(3)	C-1–C-2	1.517(5)
Eu-1–O-8	2.443(3)	C-2–C-3	1.510(5)
Eu-1–O-9	2.474(3)	C-3–C-3 # 1	1.531(7)
Eu-1–O-2	2.498(3)		
Bond angles			
O-7–Eu-1–O-5	70.94(11)	O-6–Eu-1–O-2	143.62(11)
O-7–Eu-1–O-6	77.89(11)	O-3–Eu-1–O-2	63.69(8)
O-5–Eu-1–O-6	84.09(12)	O-4–Eu-1–O-2	121.49(10)
O-7–Eu-1–O-3	131.63(10)	O-8–Eu-1–O-2	113.02(10)
O-5–Eu-1–O-3	84.29(10)	O-9–Eu-1–O-2	128.36(11)
O-6–Eu-1–O-3	141.26(10)	O-7–Eu-1–O-1	98.42(12)
O-7–Eu-1–O-4	131.78(11)	O-5–Eu-1–O-1	133.56(10)
O-5–Eu-1–O-4	70.08(11)	O-6–Eu-1–O-1	139.36(11)
O-6–Eu-1–O-4	70.95(11)	O-3–Eu-1–O-1	69.44(10)
O-3–Eu-1–O-4	70.34(10)	O-4–Eu-1–O-1	129.11(12)
O-7–Eu-1–O-8	73.44(11)	O-8–Eu-1–O-1	70.43(10)
O-5–Eu-1–O-8	139.36(11)	O-9–Eu-1–O-1	72.81(12)
O-6–Eu-1–O-8	69.78(11)	O-2–Eu-1–O-1	62.98(10)
O-3–Eu-1–O-8	135.16(10)	C-1–O-1–Eu-1	120.7(2)
O-4–Eu-1–O-8	125.02(11)	C-2–O-2–Eu-1	110.37(19)
O-7–Eu-1–O-9	145.95(11)	C-3–O-3–Eu-1	122.56(19)
O-5–Eu-1–O-9	138.62(10)	O-1–C-1–C-2	108.7(3)
O-6–Eu-1–O-9	87.78(13)	O-2–C-2–C-3	104.9(3)
O-3–Eu-1–O-9	77.15(11)	O-2–C-2–C-1	108.4(3)
O-4–Eu-1–O-9	68.91(11)	C-3–C-2–C-1	114.6(3)
O-8–Eu-1–O-9	72.63(11)	O-3–C-3–C-2	106.9(3)
O-7–Eu-1–O-2	69.12(10)	O-3–C-3–C-3 # 1	107.9(3)
O-5–Eu-1–O-2	71.21(10)	C-2–C-3–C-3 # 1	112.8(3)

Symmetry transformations used to generate equivalent atoms: # 1 $-x+1$, $-y+2$, $-z+1$.

Table 8
Hydrogen bonds with $H\cdots A < r(A)+2.000$ Å and $\angle DHA > 110°$ for $2EuCl_3 \cdot C_6H_{14}O_6 \cdot 14\ H_2O$

D-H···A	d(D–H)	d(H···A)	d(D···A)	∠(DHA)
O-1–H-11···Cl-2 # 2	0.75(8)	2.45(8)	3.181(3)	164(8)
O-2–H-12···Cl-1 # 3	0.70(7)	2.37(7)	3.031(3)	160(8)
O-3–H-13···O-10	0.68(7)	1.98(7)	2.657(5)	174(9)
O-4–H-14A···Cl-2 # 4	0.73(8)	2.39(8)	3.117(3)	171(8)
O-4–H-14B···Cl-1 # 5	0.76(8)	2.35(8)	3.102(3)	168(8)
O-5–H-15A···Cl-1 # 5	0.73(8)	2.43(8)	3.148(3)	168(8)
O-5–H-15B···Cl-3	0.75(8)	2.45(8)	3.167(3)	163(8)
O-6–H-16A···Cl-3 # 5	0.88(2)	2.26(2)	3.138(3)	173(7)
O-6–H-16B···Cl-2	0.89(2)	2.42(2)	3.299(3)	169(6)
O-7–H-17A···Cl-1	0.87(8)	2.25(8)	3.110(3)	170(7)
O-7–H-17B···Cl-3 # 3	0.84(8)	2.29(8)	3.112(3)	164(7)
O-8–H-18A···Cl-3 # 6	0.83(8)	2.33(8)	3.155(3)	170(7)
O-8–H-18B···Cl-2 # 2	0.65(8)	2.51(8)	3.151(3)	173(9)
O-9–H-19A···Cl-2 # 4	0.89(2)	2.46(3)	3.308(4)	159(6)
O-9–H-19B···O-10 # 7	0.69(8)	2.36(8)	3.037(6)	165(8)
O-10–H-20A···Cl-2 # 8	0.83(8)	2.53(8)	3.296(4)	153(7)

Symmetry transformations used to generate equivalent atoms: # 1 $-x+1$, $-y+2$, $-z+1$; # 2 $-x$, $-y+1$, $-z$; # 3 $-x+1$, $-y+1$, $-z$; # 4 $-x$, $-y+1$, $-z+1$; # 5 $-x+1$, $-y+1$, $-z+1$; # 6 $x-1$, y, z; # 7 $-x$, $-y+2$, $-z+1$; # 8 x, $y+1$, $z+1$.

indicate similar structures. The original IR spectra of Ca–, Eu–, Dy–, and Er–galactitol complexes in the 4000–650 cm^{-1} region are shown in Fig. 5. The IR and Raman spectra data in the 1500–650 cm^{-1} region and preliminary assignments, are listed in Table 9. The IR spectra of Pr–, Nd–, Sm–, Eu–, Dy–, and Er–galactitol complexes in the whole region are very similar, showing that Dy^{3+}, and Er^{3+} must have the same coordination mode, as with Pr^{3+}, Nd^{3+}, Sm^{3+}, and Eu^{3+}: lanthanide ions coordinate to nine oxygen atoms, three from the alditol and six from water molecules; each galactitol provides O-1, -2, -3 to coordinate with one lanthanide ion and O-4, -5, -6 with another lanthanide ion; another two water molecules are hydrogen-bonded in the structures and thus the formulas are $2LnCl_3 \cdot$galactitol$\cdot 14\ H_2O$. The IR spec-

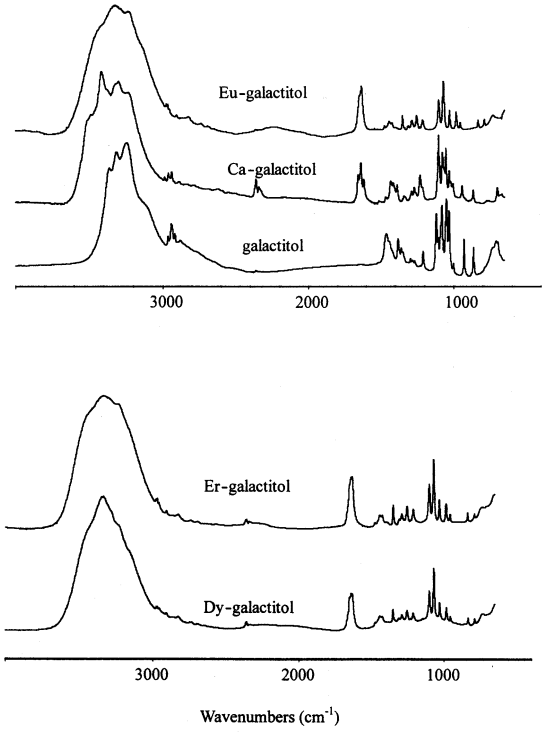

Fig. 5. The IR spectra of Ca–, Eu–, Dy–, Er–galactitol complexes.

Table 9
The IR and Raman spectra data of galactitol (G) and its metal complexes (MG) in the 1500–650 cm^{-1} region and preliminary assignments

IR					Raman			Assignments[19–21]
G	CaG	EuG	DyG	ErG	G	CaG	EuG	
1459	1463	1471	1472	1473	1464	1462	1473	νCC, νCO, τCCCH
1438	1428	1439	1438	1439	1429			νCC, δCCO, δCCH, τHCCC
	1412	1420	1421	1422	1400	1401		νCC, νCO, δCCH, τCCCH
1379	1385	1395		1391	1379	1382	1376	νCC, νCO, δCCO, δCCH, δCOH, τCCCO
1357	1337	1347	1346	1346	1343			δOCH, δCCH, δCOH, νCO
		1308	1307	1305	1320	1322	1321	δCOH, τCCCO
1295						1293		
1280	1286	1283	1285	1286	1270	1268	1279	δCOH, νCC,νCO
1266	1268	1251	1251	1251	1249			νCC, δOCH, δCCH
	1229	1228	1227	1226		1227	1228	
1209	1214	1211	1210	1209				
1118	1157				1155	1133	1128	νCO, τCCCC, τCCCO, νCC
1104	1102	1100	1099	1099	1105	1112	1110	νCO, τCCCC, τCCCO
1079	1075	1068	1068	1068	1081	1073		νCO, νCC
	1065						1066	
1049	1052				1059			
1031	1030	1027	1029	1030			1039	νCO, νCC
	1020							
1001	1004	980	982	984	1001	999	970	νCO, τCCCO
927	942	953	955	956				νCC, τCCCO, τOCCH
908	925				908	925	932	νCC, νCO
	889				878	893	891	νCC, νCO, τOCCH
863	865	831	834	836				νCC, νCO, τCCCO, τHCCO
	774	788	790	792	789	776		νCC, νCO, τOCCC, τOCCH
	756							
709	700	727	735					δCCO
697	669							

trum of $CaCl_2$·galactitol·4 H_2O is different from those of Pr–, Nd–, Sm–, Eu–, Dy–, and Er–galactitol, which is also consistent with the crystal structure results (see Fig. 5 and Table 9). The results of the spectral analysis are described in the following section.

The peaks in the 4000–3000 cm^{-1} region may be assigned to the stretching vibrations of OH of the alditol and water OH stretching vibrations influenced by extensive hydrogen-bond networks. For lanthanide–galactitol complexes, each spectrum has a broad band; for the Ca–galactitol complex, several peaks appear in the region and show more detail than the spectra of lanthanide complexes, maybe related to the hydrogen-bond data (Tables 4 and 8). The Eu–galactitol complex has more hydrogen bonds and the O–H···O(Cl) hydrogen-bond distances are approximately centralized at 3.1 Å, but for the Ca–galactitol complex, hydrogen-bond distances can be assigned to several groups, and several peaks appear in the IR spectrum of the corresponding Ca–galactitol complex.

In the 3000–2500 cm^{-1} region, the weak peaks in those complex spectra could be assigned to CH stretching vibrations. After complexation, these bands assigned to CH stretching vibrations are shifted and their relative intensities are decreased. The OH vibrations mask the CH bands.

The medium bands at $\sim$1640 cm^{-1} (due to water bending mode) in the 1700–1500 cm^{-1} region, which are absent from the spectrum of the free sugar, are assigned to bonded water molecules. Three peaks appear in the 1700–1500 cm^{-1} region in the spectrum of the Ca–galactitol complex: 1655, 1636 and 1615 cm^{-1}, corresponding to various water molecules in the structure. For lanthanide complexes, the peak can also be split into more peaks according to curve-fitting results.[9]

In the 1500–650 cm^{-1} region, five characteristic peaks ($\sim$1099, $\sim$1068, $\sim$1027, $\sim$980, $\sim$953 cm^{-1}) appear in the spectra of the lanthanide complexes. The peaks in this region may be assigned to deformation vibrations of HCH, CH_2OH; CO, and CC stretching vibrations; deformational vibration of COH, CCH, OCH, CCO, CCC, and so on.[19–21] After complexation the peaks are shifted and the relative intensities are changed corresponding to the changes in bond dis-

tances and bond angles of the structure and indicating conformational changes of the sugar molecule. Various lanthanide ion complexes, namely Pr^{3+}–, Nd^{3+}–, Sm^{3+}–, Eu^{3+}–, Dy^{3+}–, and Er^{3+}–galactitol complexes, show five similar peaks in the region, indicating that the skeletal vibrations of galactitol are similar for the six lanthanide complexes (see Fig. 5 and Table 9). The conclusion from these IR spectra is that the six metal ions have the same coordination mode to galactitol and the structures of the Dy^{3+}–, and Er^{3+}–galactitol complexes are similar to those of the others. The spectrum of Ca–galactitol is different from these lanthanide complexes in respects to relative intensities and peak positions. For example, the position of the strongest peak in the region is 1102 cm^{-1} for Ca–galactitol and $\sim$ 1068 cm^{-1} for the lanthanide complexes (see Fig. 5 and Table 9). The results show that Ca–galactitol and Ln–galactitol complexes have different coordination structures. This conclusion is consistent with the crystal structures, which indicate that the molar ratio of metal ion to ligand is 1:1 for the Ca–galactitol complex and 2:1 for lanthanide–galactitol complexes.

The FIR spectra of galactitol and its Ca, Eu, and Dy complexes are shown in Fig. 6. It is quite difficult to locate a certain absorption band in the low-frequency region to assign with certainty to M–O (sugar) stretching mode. This low frequency region is obscured by

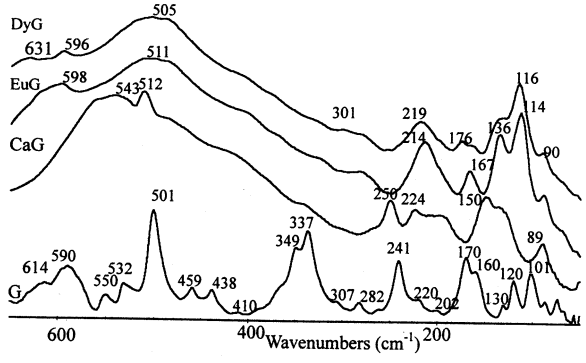

Fig. 6. The FIR spectra of galactitol and its Ca–, Eu–, Dy–complexes.

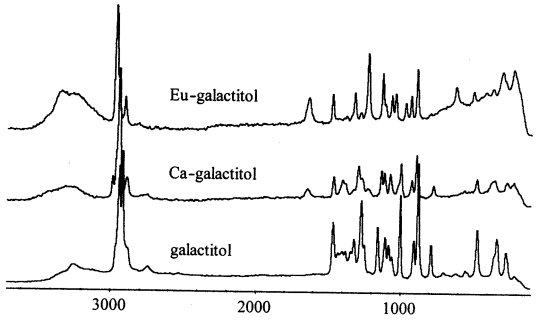

Fig. 7. The Raman spectra of Ca–, Eu–galactitol complexes.

several bands related to lattice vibrations and also M–O (H_2O) modes. According to the literature,[22] bands at $\sim$200 cm^{-1} are regarded as M–O vibrations, and therefore, 219 cm^{-1} for Dy–galactitol and a 214 cm^{-1} band for Eu–galactitol belong to M–O vibrations, providing one of the most important items of evidence for complex formation.

Raman spectroscopic study of Ca–, and Eu –galactitol complexes.—The Raman spectra of Ca– and Eu–galactitol are shown in Fig. 7. The spectra data in the 1500–650 cm^{-1} region are listed in Table 9. IR and Raman spectra provide complementary information. Here, the Raman spectra show larger differences in peak positions and relative intensities than the corresponding IR spectra for these lanthanide complexes.[10] A broad band of OH stretching vibrations appears in the 3700–3000 cm^{-1} region in each spectrum. The bands for CH stretching vibrations fall within the 3000–2500 cm^{-1} region: 2987, 2944, 2891 cm^{-1} for the Ca–galactitol complex and 2965, 2946, and 2905 cm^{-1} for the Eu–galactitol complex. Compared with the corresponding IR spectra, the relative intensities of νOH vibrations are decreased, but the relative intensities of νCH vibrations are increased and become the strongest peaks in each Raman spectrum.

In the 1700–1500 cm^{-1} region, the following peaks could be assigned to the deformational vibration of water (coordinated water molecules and hydrogen-bonded water): 1643 cm^{-1} for Ca–galactitol, and 1636 cm^{-1} for the Eu–galactitol complex. In the 1500–650 cm^{-1} region the strongest peak in the spectrum of galactitol appears at 878 cm^{-1}, which could be assigned to the stretching vibration of CC and CO.[21] In the spectra of the Ca–, and Eu–complexes the peak is shifted to higher wavenumber: 893 cm^{-1} (Ca), 891 cm^{-1} (Eu) and the relative intensities to νCH have decreased. For the Ca complex, this peak is still the strongest one in this region, but for the Eu complex, the 1228 cm^{-1} peak becomes the strongest in the region. Many other peaks are also shifted to higher or lower wavenumber in the two Raman spectra. The shift to higher or lower wavenumber depends on the change in the structures related to the vibrational mode of the peak. For example, 1081 cm^{-1} is mainly the contribution of νC-6–O-6 vibrations for free galactitol and the C-6–O-6 distance become longer after complexation, and therefore, it is shifted to lower wavenumber.[10] In the 650–100 cm^{-1} region, those peaks could be assigned to M–O vibrations: 219 cm^{-1} for the Ca complex and 224 cm^{-1} for the Eu complex.[22] This is also important evidence for complex formation.

These IR and Raman results indicate the hydroxyl groups of galactitol participate in the coordination to metal ions; Ca^{2+} and Ln^{3+} have different coordination modes to galactitol; the hydrogen-bond networks rearrange after complexation; and the conformation of the

galactitol skeleton is changed upon sugar metalation. Therefore, the IR and Raman results are consistent with the crystal structures.

Considering our previous results concerning Nd, and Sm galactitol, Pr–, Nd–*myo*-inositol, Pr–D-ribose complexes, and the crystal structures reported in the literature,[6,7] one or more water molecules take part in metal ion–oxygen interaction. Therefore, the appearance of the deformation vibrations of water molecules in the IR and Raman spectra is evidence for complex formation. Because single crystals of metal–carbohydrate complexes are difficult to prepare, IR, Raman and other techniques are needed in combination to deduce unknown structures.

Acknowledgements

The authors thank the National Natural Science Foundation of China for the grants (No. 29671002, 39730160, 20023005 and 59953001) and the State Key Project for Fundamental Research of MOST (G1998061307) for support of this work.

References

1. Gyurcsik B.; Nagy L. *Coord. Chem. Rev.* **2000**, *203*, 81–148.
2. Predki P. F.; Whitfield D. M.; Sarkar B. *Biochem. J.* **1992**, *281*, 835–841.
3. Weis W. I.; Drickamer K.; Hendrickson W. A. *Nature* **1992**, *360*, 127–134.
4. Piarulli U.; Rogers A. J.; Floriani C.; Gervasio G.; Viterbo D. *Inorg. Chem.* **1997**, *36*, 6127–6133.
5. Weiss L. *J. Natl. Cancer Inst.* **1973**, *50*, 3–19.
6. Dheu-Andries M. L.; Pérez S. *Carbohydr. Res.* **1983**, *124*, 324–332.
7. Cook, W. J.; Bugg, C. E. In *Metal–Ligand Interactions in Organic Chemistry and Biochemistry*, *Part* 2; Pullman, B.; Goldblum, N., Eds.; Reidel: Dordrecht, Holland, 1977; pp 231–256.
8. Angyal S. J.; Craig D. C. *Carbohydr. Res.* **1993**, *241*, 1–8.
9. Yang L. M.; Zhao Y.; Tian W.; Jin X. L.; Weng S. F.; Wu J. G. *Carbohydr. Res.* **2001**, *330*, 125–130.
10. Yang L. M.; Tian W.; Zhao Y.; Jin X. L.; Weng S. F.; Wu J. G.; Xu G. X. *J. Inorg. Biochem.* **2001**, *83*, 161–167.
11. Israeli Y.; Morel J.-P.; Morel-Desrosiers N. *Carbohydr. Res.* **1994**, *263*, 25–33.
12. Chen Z.; Morel-Desrosiers N.; Morel J.-P.; Detellier C. *Can. J. Chem.* **1994**, *72*, 1753–1757.
13. Angyal S. J. *Adv. Carbohydr. Chem. Biochem.* **1989**, *47*, 1–43.
14. Yang L. M.; Wang Z. M.; Zhao Y.; Tian W.; Jin X. L.; Xu Y. Z.; Weng S. F.; Wu J. G. *Carbohydr. Res.* **2000**, *329*, 847–853.
15. Yang L. M.; Tao D. L.; Sun Y.; Jin X. L.; Zhao Y.; Yang Z. L.; Weng S. F.; Wu J. G.; Xu G. X. *J. Mol. Struct.* **2001**, *560*, 105–113.
16. Yang L. M.; Zhao Y.; Xu Y. Z.; Jin X. L.; Weng S. F.; Tian W.; Wu J. G.; Xu G. X. *Carbohydr. Res.* **2001**, *334*, 91–95.
17. Jeffrey G. A.; Kim H. S. *Carbohydr. Res.* **1970**, *14*, 207–216.
18. Berman H. M.; Rosenstein R. D. *Acta Crystallogr., Sect. B* **1968**, *24*, 435–441.
19. Mathlouthi M.; Koenig J. L. *Adv. Carbohydr. Chem. Biochem.* **1986**, *44*, 7–89.
20. Zhbankov R. G.; Andrianov V. M.; Ratajczak H.; Marchewka M. *Zh. Strukt. Khim.* **1995**, *36*, 430–442.
21. Zhbankov R. G. *J. Mol. Struct.* **1992**, *275*, 65–84.
22. Yang L. Q.; Wu J. G.; Zhou Q.; Bian J.; Yang Y. M.; Xu D. F.; Xu G. X. *Microchim. Acta* **1997**, *14*, 251–252.